

State transfer and entanglement betweentwo- and four-level atoms in a cavity

Si-Wu Li(李思吾), Tianfeng Feng(冯田峰), Xiao-Long Hu(胡骁龙), and Xiaoqi Zhou(周晓祺)
Citation: Chin. Phys. B, 2023, 32 (**10**): 104214. DOI: 10.1088/1674-1056/acf205
Journal homepage: http://cpb.iphy.ac.cn; http://iopscience.iop.org/cpb

What follows is a list of articles you may be interested in

Nonreciprocal coupling induced entanglement enhancement in a double-cavity optomechanical system

Yuan-Yuan Liu(刘元元), Zhi-Ming Zhang(张智明), Jun-Hao Liu(刘军浩), Jin-Dong Wang(王金东), and Ya-Fei Yu(於亚飞)
Chin. Phys. B, 2022, 31 (**9**): 094203. DOI: 10.1088/1674-1056/ac6499

Bright 547-dimensional Hilbert-space entangled resource in 28-pair modes biphoton frequency comb from a reconfigurable silicon microring resonator

Qilin Zheng(郑骑林), Jiacheng Liu(刘嘉成), Chao Wu(吴超), Shichuan Xue(薛诗川), Pingyu Zhu(朱枰谕), Yang Wang(王洋), Xinyao Yu(于馨瑶), Miaomiao Yu(余苗苗), Mingtang Deng(邓明堂), Junjie Wu(吴俊杰), and Ping Xu(徐平)
Chin. Phys. B, 2022, 31 (**2**): 024206. DOI: 10.1088/1674-1056/ac3507

Quantum speed limit time and entanglement in a non-Markovian evolution of spin qubits of coupled quantum dots

M. Bagheri Harouni
Chin. Phys. B, 2020, 29 (**12**): 124203. DOI: 10.1088/1674-1056/abab75

Reversion of weak-measured quantum entanglement state

Shao-Jiang Du(杜少将), Yonggang Peng(彭勇刚), Hai-Ran Feng(冯海冉), Feng Han(韩峰), Lian-Wu Yang(杨连武), Yu-Jun Zheng(郑雨军)
Chin. Phys. B, 2020, 29 (**7**): 074202. DOI: 10.1088/1674-1056/ab8c3e

Quantum state transfer via a hybrid solid-optomechanical interface

Pei Pei(裴培), He-Fei Huang(黄鹤飞), Yan-Qing Guo(郭彦青), Xing-Yuan Zhang(张兴远), Jia-Feng Dai(戴佳峰)
Chin. Phys. B, 2018, 27 (**2**): 024203. DOI: 10.1088/1674-1056/27/2/024203

State transfer and entanglement between two- and four-level atoms in a cavity

Si-Wu Li(李思吾), Tianfeng Feng(冯田峰), Xiao-Long Hu(胡骁龙), and Xiaoqi Zhou(周晓祺)†

School of Physics, Sun Yat-Sen University, Guangzhou 510275, *China*

(Received 7 July 2023; revised manuscript received 4 August 2023; accepted manuscript online 21 August 2023)

Qudits with a large Hilbert space to host quantum information are widely utilized in various applications, such as quantum simulation and quantum computation, but the manipulation and scalability of qudits still face challenges. Here, we propose a scheme to directly and locally transfer quantum information from multiple atomic qubits to a single qudit and vice versa in an optical cavity. With the qubit–qudit interaction induced by the cavity, our scheme can transfer quantum states efficiently and measurement-independently. In addition, this scheme can robustly generate a high-dimensional maximal entangled state with asymmetric particle numbers, showing its potential in realizing an entanglement channel. Such an information interface for qubits and qudit may have enlightening significance for future research on quantum systems in hybrid dimensions.

Keywords: quantum state transfer, quantum entanglement, cavity quantum eletrodynamics

PACS: 42.50.–p, 42.50.Dv, 03.67.–a **DOI:** 10.1088/1674-1056/acf205

1. Introduction

At present, most theories and experiments about quantum information are based on two-level systems, so-called qubits. However, in the microscopic world, atoms,[1–3] photons,[4–6] and solid-state systems[7–9] actually possess more than two eigenstates, which allows us to store and handle d-dimensional quantum information in a single qubit named qudits. Compared to qubits, such systems have exponentially increased information capacity and show enormous potential in constructing high-dimensional quantum gates to boost the performance of quantum computation.[10–12] Qudits can also locally implement complex Hamiltonian in quantum simulations, such as the discovery of new gauge fields for new physics,[13,14] and quantum chemical dynamics involving molecular or atomic vibrations.[15] Furthermore, one can use qudit systems to realize entanglement in more complex structures[16–18] and stronger Bell non-locality,[19] and to explore the boundaries of entanglement of physical systems.

In order to manipulate qudits, coupling well-studied qubits to qudits is a promising way. Thus, it is necessary to study the connection and state transfer between the particles with different dimensions, such as multiple qubits and qudits, in a hybrid-dimensional system.[20] Recently, various approaches were proposed to implement state transfer in the same-dimensional system by employing the cavity-assisted Raman process[21,22] and resonant cavities,[23,24] which all require cavities with high quality factors. Besides, the direct interaction between qubits can also be used to realize state transfer without the restriction of the cavity's quality,[25] and it is widely adopted in the solid-state quantum system for fast and scalable quantum information processing. Inspired by these schemes, constructing the interaction between qubits and qudits in quantum electrodynamics (QED),[26–28] which describes photon–atom or atom–atom interaction and has been used to realize quantum logic operations,[29–31] can also achieve the state transfer. Moreover, long-distance quantum teleportations[32–34] are based on quantum entanglement channels, and those entangled states are also prepared in same-dimensional quantum objects. Researchers have proposed a number of schemes to prepare entanglements between atoms in QED systems.[35–37] To realize a possible quantum teleportation communication channel, we can also utilize QED to generate a special entanglement in a hybrid-dimensional quantum system.

In this paper, we propose a cavity QED-based scheme to construct photon-induced qubit–ququart interaction that enables us to implement quantum state transfer between two qubits and a single ququart. Using this coherent interaction and photon-number-dependent shift, arbitrary states in two qubits can be encoded into the ququart and vice versa with high-fidelity. Our proposed scheme can also be used to robustly and noise-resistantly generate a maximum entanglement between two-dimensional and four-dimensional systems, i.e., to prepare an asymmetric maximally entangled state (the AMES or (2, 2, 4) entangled state).[38] Such an entangled state can be potentially used to establish a teleportation interface for atoms possessing different levels. Unlike previous implementations on linear optics, our approach can prepare the (2, 2, 4) entangled state efficiently and determinately. We believe our scheme can be extended to the case of multiple qubits and qudits of more dimensions as the structural complexity of the

†Corresponding author. E-mail: zhouxq8@mail.sysu.edu.cn

© 2023 Chinese Physical Society and IOP Publishing Ltd

light fields increases.

Our paper is organized as follows. In Section 2, we introduce the system of the proposed scheme and derive an effective Hamiltonian for transferring the information between hybrid-dimensional systems. Then we discuss the state-transfer process in two different cases with or without the AC-Stark phase shift. Section 3 further studies how to utilize a modified system to prepare AMES in high fidelity. In addition, Section 4 presents some discussions on our schemes, such as the error from system's imperfection and the influence of decoherence in the system. Finally, we make a conclusion for our state transfer and entanglement preparation scheme, and a vision of the future.

2. Coherent state transfer between two qubits and a ququart

2.1. The model

Our target is to construct a cavity QED system, in which quantum information can be transferred from two qubits to a ququart, i.e.,

$$\begin{aligned} &|\psi_{0,1}\rangle = (C_{gg}|gg\rangle + C_{eg}|eg\rangle + C_{ge}|ge\rangle + C_{ee}|ee\rangle)\otimes|1\rangle \\ \rightarrow\ &|\psi_{\rm tar}\rangle = |gg\rangle\otimes(C_{gg}|1\rangle + C_{ge}|2\rangle + C_{eg}|3\rangle + C_{ee}|4\rangle), \end{aligned} \quad (1)$$

where the first and second entries in the kets represent states of qubits A and B, respectively, while the third entry represents the states of the ququart.

We consider a system consisting of two qubits and one ququart coupled with the same cavity via two orthogonal polarized photonic modes a and b, whose exciting frequencies are $\omega_{\rm ca}$. The atomic qubits have transition dipoles with degenerate excited frequencies $\omega_{\rm at}$, and couple to modes a and b, respectively. The single ququart atom possesses two single-exciton states and one biexciton state, whose transitions also interact with two cavity modes. Figure 1 depicts the level structures of qubits and the ququart. The system's Hamiltonian can be written as (throughout the paper, $\hbar = 1$)

$$\begin{aligned} H &= H_0 + H_{\rm I}, \\ H_0 &= \omega_{\rm ca} a^\dagger a + \omega_{\rm at}(\sigma_{\rm A}^\dagger\sigma_{\rm A} + |2\rangle\langle 2| + |4\rangle\langle 4|) \\ &\quad + \omega_{\rm ca} b^\dagger b + \omega_{\rm at}(\sigma_{\rm B}^\dagger\sigma_{\rm B} + |3\rangle\langle 3| + |4\rangle\langle 4|), \\ H_{\rm I} &= g_{\rm A}(a^\dagger D_{\rm A} + D_{\rm A}^\dagger a) + g_{\rm B}(b^\dagger D_{\rm B} + D_{\rm B}^\dagger b). \end{aligned} \quad (2)$$

Here, we consider a Jaynes–Cummings type interaction between multiple atoms and cavity modes with coupling strengths $g_{\rm A}$ and $g_{\rm B}$, respectively, which are identical for the same polarization. The collective dipole operators read

$$D_{\rm A} = \sigma_{\rm A} + |1\rangle\langle 2| + |3\rangle\langle 4|, \quad D_{\rm B} = \sigma_{\rm B} + |1\rangle\langle 3| + |2\rangle\langle 4|, \quad (3)$$

where $\sigma_n = |g\rangle_n\langle e|_n$, which is the lower operator of the two-level system.

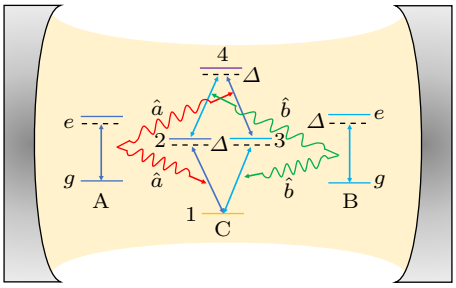


Fig. 1. Sketch of the atomic level structure and coupling field mode in our proposed scheme. Two-level atoms A and B interact with polarized field modes a (red arrow) and b (green arrow) respectively. The four-level atom contains orthogonal transition dipoles interacting with polarized field modes.

When the energy of the cavity fields does not match the exciting energy of the atomic system, the effective interaction would be weakened, and there is no energy exchange between them. Cavity modes can be virtually excited, and the second-order interaction dominates the system's dynamics, where qubits and the ququart exchange their excitations. In this case, we can use this cavity QED model to implement the quantum state transfer, while the decoherence of the cavity is suppressed. We perform the Schrieffer–Wolf transformation[39]

$$U = \exp\left[-\frac{g_{\rm A}}{\Delta}(D_{\rm A}^\dagger a - a^\dagger D_{\rm A}) - \frac{g_{\rm B}}{\Delta}(D_{\rm B}^\dagger b - b^\dagger D_{\rm B})\right] \quad (4)$$

on H to adiabatically eliminate cavity modes in the system's evolution, where the detuning satisfies $\Delta = |\omega_{\rm ca} - \omega_{\rm at}| \gg g_{\rm A}$, $g_{\rm B}$. After the transformation, the effective Hamiltonian of the system becomes

$$H_{\rm eff} = H_0 - \frac{g_{\rm A}^2}{\Delta}\left[D_{\rm A}^\dagger D_{\rm A} + D_{\rm A}^z a^\dagger a\right] - \frac{g_{\rm B}^2}{\Delta}\left[D_{\rm B}^\dagger D_{\rm B} + D_{\rm B}^z b^\dagger b\right], \quad (5)$$

where

$$\begin{aligned} D_{\rm A}^z &= \sigma_{\rm A}^\dagger\sigma_{\rm A} - \sigma_{\rm A}\sigma_{\rm A}^\dagger + |4\rangle\langle 4| - |3\rangle\langle 3| + |2\rangle\langle 2| - |1\rangle\langle 1|, \\ D_{\rm B}^z &= \sigma_{\rm B}^\dagger\sigma_{\rm B} - \sigma_{\rm B}\sigma_{\rm B}^\dagger + |4\rangle\langle 4| - |2\rangle\langle 2| + |3\rangle\langle 3| - |1\rangle\langle 1|. \end{aligned} \quad (6)$$

The second and fourth terms in Eq. (5) describe the qubit–ququart interaction, while the third and fifth terms denote the photon-number-dependent shift.

With the effective coupling strength, $\lambda \equiv -g_{\rm A}^2/\Delta = -g_{\rm B}^2/\Delta$ and the photon-number-dependent phase shift in $H_{\rm eff}$, this cavity QED system can achieve the state transfer. First, we assume that a and b modes initially are both in vacuum states so that the effective Hamiltonian in Eq. (5) can be projected into the photon-vacuum subspace, i.e.,

$$H_{\rm eff,vac} = H_0 + \lambda(D_{\rm A}^\dagger D_{\rm A} + D_{\rm B}^\dagger D_{\rm B}). \quad (7)$$

Because Eq. (1) contains states in different subspaces with the particle-exchange interaction, the state evolution could be written as

$$|\psi(t)\rangle = C_{gg}|gg1\rangle + C_{eg}\left[\alpha_{eg}(t)|eg1\rangle + \beta_{eg}(t)|gg2\rangle\right]$$

$$+C_{ge}\left[\alpha_{ge}(t)|ge1\rangle+\beta_{ge}(t)|gg3\rangle\right]$$
$$+C_{ee}\left[\alpha_{ee}(t)|ee1\rangle+\beta_{ee}(t)|ge2\rangle\right.$$
$$\left.+\theta_{ee}(t)|eg3\rangle+\mu_{ee}(t)|gg4\rangle\right], \quad (8)$$

where $\alpha_{\mu\nu}$ and $\beta_{\mu\nu}$ represent normalized amplitudes for their corresponding subspaces. Note that we have omitted the cavity's degree of freedom. With $H_{\text{eff,vac}}$, the two-qubit state will be transferred to the ququart at $t=\pi/(2\lambda)$,

$$|\psi(\frac{\pi}{2\lambda})\rangle = \exp\left(-\mathrm{i}H_{\text{eff,vac}}\frac{\pi}{2\lambda}\right)|\psi_{0,1}\rangle$$
$$= |gg\rangle\otimes(C_{gg}|1\rangle-C_{eg}|2\rangle-C_{ge}|3\rangle+C_{ee}|4\rangle). \quad (9)$$

It indicates additional minus signs in the final state, which will noticeably decrease the transfer fidelity. For correcting these minus signs, single-qubit phase operations on qubits A and B should be performed, respectively, before the cavity-induced interaction. Then the cavity QED model without the photonic excitation implements the local state-transfer operation with high fidelity.

Furthermore, using the photon-number-dependent phase shift, the system can also achieve a high-fidelity state transfer without single-qubit operations. Initially, the double-mode single-photon state is prepared in the cavity, and H_{eff} in the single-photon subspace is given by

$$H_{\text{eff,ph}}=H_0+\lambda(D_{\text{A}}^{\dagger}D_{\text{A}}+D_{\text{B}}^{\dagger}D_{\text{B}}+D_{\text{A}}^{z}+D_{\text{B}}^{z}). \quad (10)$$

The final state of the evolution is

$$|\psi'(\frac{\pi}{2\lambda})\rangle = \exp(-\mathrm{i}H_{\text{eff,ph}}\frac{\pi}{2\lambda})|\psi_{0,1}\rangle$$
$$= |gg\rangle\otimes(C_{gg}|1\rangle+C_{eg}|2\rangle+C_{ge}|3\rangle+C_{ee}|4\rangle). \quad (11)$$

Finally, a state transfer is realized without performing local qubit operations before the atomic interaction. It is worth mentioning that the effective Hamiltonian requires double-mode single-photon state preparation in the cavity. It is possible to experimentally prepare this single-photon state by exploiting resonant emitters coupling to the cavity.[40,41] Using optical exciting by classical fields on the emitters, the cavity will absorb the excitation of resonant emitters and be in the double-mode one-photon state after the relaxation. However, it introduces additional complexities and makes the state transfer more challenging. In comparison, the vacuum cavity can achieve the state transfer without the need for pre-state preparation, albeit it requires convenient single-qubit operations. Moreover, an ultrahigh-Q cavity is demanded in the double-mode single-photon case to handle photonic loss, while the virtual excitation in the vacuum-cavity case enhances the coherent time of the cavity.

Figure 2 reveals the states' evolution with the Hamiltonian $H_{\text{eff,ph}}$, which contains the single-photon phase shift. At the initial time, $\alpha_{ge}=\alpha_{eg}=\alpha_{ee}=1$, and the two-qubit system is separated from the ququart. After a period of time, two systems are entangled and then are separated again at $t=\pi/(2\lambda)$, while the amplitude information, initially encoded in the two-qubit system, has been transferred to the single-ququart system. The time-dependent fidelity of the state transfer process defined as $|\langle\psi(t)||\psi(T)\rangle|^2$ is also shown in Fig. 2. The fidelity reaches the maximal value when $t=\pi/(2\lambda)$ along the system's evolution. The amplitude information is transferred back to the qubits after $t=\pi/(2\lambda)$, and it means that the inverse state transfer process can also be achieved with this approach. Note that four terms in Fig. 2 sufficiently represent the process of state transfer in Eq. (8) owing to the symmetry of the system's Hamiltonian ($g_{\text{A}}=g_{\text{B}}$).

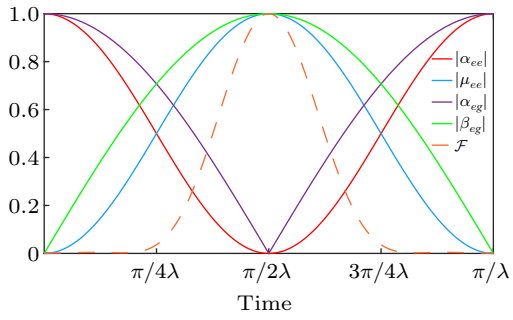


Fig. 2. Time-dependent Rabi-type oscillation of the state transfer between 2 qubits and a ququart, with the system's Hamiltonian $H_{\text{eff,ph}}$. The transfer time is identical to single- and double-excitation subspaces, and amplitudes (solid lines) are transferred synchronously. The fidelity (orange dashed line), $\mathcal{F}$, indicates the phase difference between the transferred state and the ideal state.

In a 2 to 1 state transfer process, one can implement the information interface for a hybrid-dimensional system to transfer two-body information on a single particle. In a reverse process, one can prepare arbitrary whatever entanglement or not two-body quantum state after preparing a single particle state without direct interaction between low-dimensional particles.[20]

In contrast to previous schemes[20,38] that employed probabilistic gates in linear optics, our proposed scheme accomplishes state transfer using an effective qubit–ququart interaction, leading to the evolution described by Eq. (8). In other words, our proposal eliminates the need for state projection measurements, making it an efficient and deterministic approach.

In experiments, the cavity with two orthogonal polarized modes can be realized by a circular resonator[42–44] and the cavity photons possess orthogonal polarization. The diamond-type ququart has been studied and observed in Rb atoms,[45–47] and manufactured by artificial atoms such as quantum dots (QDs)[48,49] and superconducting circuits.[50,51] In the atomic case, the two atomic qubits and the atomic ququart are sent into the cavity, remaining inside the cavity for a duration of $t=\pi/(2\lambda)$,[52–55] and then the cavity-induced interaction enables the state transfer to be accomplished. In the solid-state

artificial atom case, two-qubit systems and the ququart system are embedded into a cavity, and driving fields interact with them to control the interaction between artificial atoms,[56] with the duration satisfying $t = \pi/(2\lambda)$.

2.2. The validity of the model in the far-detuning regime

With the full Hamiltonian Eq. (2), the time-dependent fidelity is defined as

$$\mathcal{F}(t) = |\langle\psi(t)||\Psi_{\rm tar}\rangle|^2, \tag{12}$$

where

$$|\Psi_{\rm tar}\rangle = |gg\rangle \otimes (C_{gg}|1\rangle + C_{ge}|2\rangle + C_{eg}|3\rangle + C_{ee}|4\rangle) \otimes |0_a 0_b\rangle. \tag{13}$$

The cavity's degrees of freedom are not eliminated in the full Hamiltonian, and the photonic Fock states are included in the time evolution. The target photonic state is vacuum, while the energy and information remain stored in the atomic system.

Figure 3(a) displays the time-dependent fidelity for the state transfer under different detunings Δ, i.e., $\Delta/g = 5$, 10, 20, 50, respectively. When the detuning presents, photons will be radiated and be quickly absorbed, resulting in a low probability of cavity excitation, $P \propto (g/\Delta)^2$. When $\Delta/g = 5$, the fidelity exhibits obvious oscillations, and it does not reach the maximum value at $\lambda t = \pi/2$ due to the excitation of the cavity modes. The approximation in Eq. (5) is unreliable because the detuning is not large enough. The oscillation is weakened as the detuning increases because of the more rapid and weaker evolution of photons. When $\Delta/g = 10$, the system achieves a fidelity of $\mathcal{F}(\pi/(2\lambda)) > 0.99$, as shown by the dark blue line in Fig. 3(a), indicating that the adiabatic elimination of cavity modes takes effect. As $\Delta/g = 20$ and $\Delta/g = 50$, the oscillation is inconspicuous, and the maximal values almost approach 100%. The maximal fidelity is mainly affected by the photon excitation, and the error is given by $1 - \mathcal{F} \propto (g/\Delta)^2$.

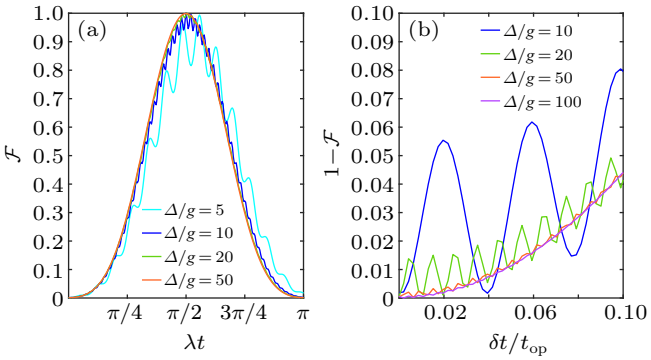


Fig. 3. (a) Time evolution of the fidelity for state transfer, using the full Hamiltonian, with different values of Δ/g, namely, 5, 10, 20, and 50, respectively. (b) The error is a function of the deviation from interaction time, and the operational time is defined as $t_{\rm op} \equiv \pi/2$.

These results demonstrate that the state transfer using the full Hamiltonian can be effectively described by the Hamiltonian given by Eq. (5) in the far-detuning regime. Specifically, for detunings satisfying $\Delta = 10g$, the system achieves a fidelity greater than 0.99. For a more stable fidelity, the detunings satisfying $\Delta = 20g$ could be better.

A high-fidelity state transfer requires accurate control of the interaction time due to the oscillation. The deviation from the intended interaction time can significantly affect the fidelity, as shown in Fig. 4(b). However, the fidelity becomes more stable with higher detuning. For instance, in the case of $\Delta = 50g$ or $\Delta = 100g$, the fidelity is still above 0.99 as long as $\Delta t/t_{\rm op} < 0.05$.

Our state-transfer scheme is accomplished by a local interaction system within a cavity, and we will expand our scheme to generate a special entanglement state, which will be discussed in Section 3.

3. The asymmetric maximal entanglement preparation

In this section, we discuss how to generate the maximal entanglement between two qubits and a ququart by exploiting the original and the modified system Hamiltonian.

To increase the scale of entangled states for more complex applications, one can increase both the number and dimensions of particles, such types of entangled states have been demonstrated.[57,58] Recently, an asymmetric maximal entangled state (AMES or (2, 2, 4) entangled state), consisting of two two-level systems and a single four-level system, i.e.,

$$\frac{1}{2}(|001\rangle + |012\rangle + |103\rangle + |114\rangle) \tag{14}$$

has been probabilistically prepared in the photonic system.[38] Because such an entangled state contains particles with different dimensions, it can be used as an interface for the information flow between quantum systems with different dimensions via the quantum state teleportation protocol.

Using our far-detuning cavity QED Hamiltonian in Eq. (7), we can prepare the atomic AMES like Eq. (14) after an evolution time, $t = \pi/(4\lambda)$, and atomic entangled state is approximately pure because the cavity is virtually excited. However, the numerical result shown in Fig. 4(a) implies that the state evolution is not stable facing the error of the temporal control when the atomic system is in the AMES.

Based on the system in Eq. (2), we introduce a frequency mismatch δ between qubits and the ququart's exciton states, and the system Hamiltonian reads

$$\begin{aligned} H_{\rm mis} &= H_{0,\rm mis} + H_{\rm I}, \\ H_{0,\rm mis} &= \omega_{\rm A}(\sigma_{\rm A}^\dagger\sigma_{\rm A} + |3\rangle\langle 3| + |4\rangle\langle 4|) + \omega_{\rm ca} a^\dagger a \\ &\quad + \omega_{\rm B}(\sigma_{\rm B}^\dagger\sigma_{\rm B} + |2\rangle\langle 2| + |4\rangle\langle 4|) + \omega_{\rm cb} b^\dagger b, \\ H_{\rm I} &= g_{\rm A}(a^\dagger D_{\rm A} + D_{\rm A}^\dagger a) + g_{\rm B}(b^\dagger D_{\rm B} + D_{\rm B}^\dagger b), \end{aligned} \tag{15}$$

where $\omega_A = \omega_{at} - \delta/2$, $\omega_B = \omega_{at} + \delta/2$, and $\delta \ll \Delta$. Again, we apply the Schrieffer–Wolf transformation $e^{S_{mis}}$ to H_{mis} and obtain an effective interaction between atoms, where

$$\begin{aligned} S_{mis} = & \frac{g_A}{\Delta}(a^\dagger \sigma_A - \sigma_A^\dagger a) + \frac{g_B}{\Delta}(b^\dagger \sigma_B - \sigma_B^\dagger b) \\ & + \frac{g_A}{\Delta - \delta/2}[a^\dagger(|1\rangle\langle 2| + |3\rangle\langle 4|) - (|2\rangle\langle 1| + |4\rangle\langle 3|)a] \\ & + \frac{g_B}{\Delta + \delta/2}[b^\dagger(|1\rangle\langle 3| + |2\rangle\langle 4|) - (|3\rangle\langle 1| + |4\rangle\langle 2|)b]. \end{aligned} \tag{16}$$

Then the final effective Hamiltonian changes to

$$H_{eff,mis} \approx H_{0,mis} - \frac{g_A^2}{\Delta - \delta/2} D_A^\dagger D_A - \frac{g_B^2}{\Delta + \delta/2} D_B^\dagger D_B, \tag{17}$$

where we have assumed that field modes are vacuum at the initial time. In the absence of frequency mismatch, the (2, 2, 4) state is always able to be generated at a certain time, no matter how the coupling strength is. When the frequency mismatch is introduced, the maximal entanglement can be prepared only as the atomic coupling is strong enough. In order to achieve the maximal entanglement, the effective coupling strength, $\lambda' \equiv g_A^2/(\Delta - \delta/2) = g_B^2/(\Delta + \delta/2)$, should satisfy

$$4\lambda'^2 \geq \delta^2. \tag{18}$$

If the equal sign holds, the initial state $|gg4\rangle$ will evolve to the AMES, saying

$$\begin{aligned} |\psi(T_e)\rangle &= \exp(-iH_{eff,mis}T_e)|gg4\rangle \\ &= \frac{1}{2}(-|ee1\rangle + |ge2\rangle - |eg3\rangle + |gg4\rangle), \end{aligned} \tag{19}$$

where the time interval $T_e = \pi/\sqrt{\delta^2 + 4\lambda'^2}$. Performing a single-qubit phase operation on qubit A, the minus signs of the first and third terms in Eq. (19) will be corrected. On the contrary, the entangled state prepared by the resonant interaction needs single-qubit operations twice to correct the additional phase, which may introduce more noise than the near-resonant case.

In Fig. 4, we show the time evolution of the preparation of AMESs. Varying $|\lambda'/\delta|$, the evolution in Figs. 4(b)–4(d) are quite different. If the frequency mismatch exists, the maximal entanglement should be conditionally prepared. As we increase λ' until it satisfies $4\lambda'^2 = \delta^2$, the AMES will be prepared with the Rabi oscillation. In Fig. 4(d), the system is in the maximal entanglement at $t = \pi/\sqrt{\delta^2 + 4\lambda'^2}$, which is the extreme point of the time evolution. It also displays that the preparation of the maximally entangled state requires less temporal-control accuracy compared to the totally resonant scheme shown in Fig. 4(a). Furthermore, the value of entangled entropy S presented in Fig. 4(d) changes very steadily around $t = \pi/\sqrt{\delta^2 + 4\lambda'^2}$.

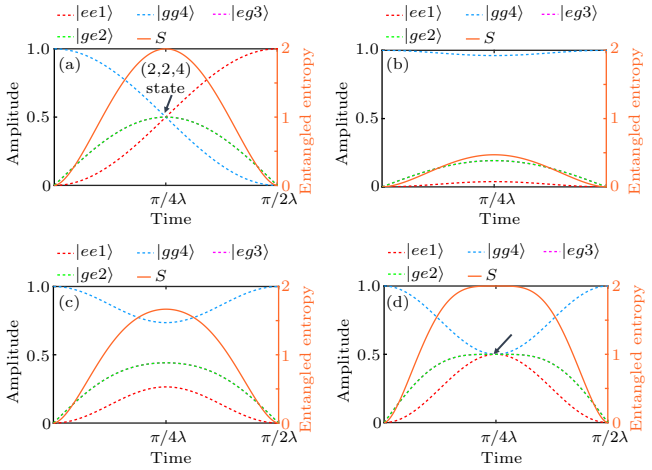


Fig. 4. Time-dependent evolution of the (2, 2, 4) entangled-state preparation (color dotted lines) and the entangled entropy S of the atomic system (orange solid lines) in the cavity QED model. Panel (a) shows the interaction process without the frequency mismatch. Panels (b)–(d) display atomic interaction processes with the frequency mismatch as the coupling strength grows, i.e., $|\lambda'/\delta| = 0.1, 0.3, 0.5$, respectively, and $\Omega = \sqrt{\delta^2 + 4\lambda'^2}$. The (2, 2, 4) state obtains as the amplitudes reach their extreme points, where the evolution is smooth and robust to the temporal error. Here, the amplitude of $|eg3\rangle$ (pink dotted lines) overlaps with $|ge2\rangle$ (green dotted lines).

In the resonant case ($\delta = 0$), the performance of information exchange between qubits and the ququart is unweakened, therefore the state transfer can be obtained at $t = \pi/(2\lambda)$. This timing corresponds to the inflection point in the evolution, ensuring a steady process. The AMES is an intermediate state and is generated at $t = \pi/(4\lambda)$, which is a fast-changing timing. When $\delta \neq 0$, it weakens the effective coupling and the information-exchange capability between qubits and the ququart. Consequently, the state transfer cannot be accomplished, and the maximal entangled entropy that the system can achieve may change with δ. For $\delta \leq 2\lambda$, the effective coupling is sufficiently strong to generate maximal entanglement ($S = 2$), even though the quantum information cannot be completely exchanged. Notably, $\delta = 2\lambda$ serves as the boundary for generating AMES at $t = \pi/\Omega$, corresponding to the inflection point of the evolution. In the case of $\delta > 2\lambda$, maximal entangled entropy of the atomic system becomes lower as δ increases due to the weaker effective coupling. Overall, a mismatch δ modulates the information-exchange capability of the atomic system and the state in the inflection point providing tardy evolution.

4. Discussion

In the previous sections, we present some analyzed results regarding the state transfer and entanglement between two- and four-level atoms using an effective Hamiltonian. However, in experimental implementations, the imperfect control of parameters and the presence of decoherence in the system can affect the three-atom operations. In this section, we will discuss these sources of errors in detail. Additionally, a gener-

alization to the higher-dimensional case will be provided using a specific Hamiltonian.

4.1. The deviation of the temporal control

The duration of the atom-cavity interaction can be controlled by the time of atoms staying in the cavity or the driving fields. However, if the control is not precise enough, the deviation in time can decrease the fidelity of the three-atom operations. In the far-detuning regime, the error of the fidelity for the state transfer can be evaluated using the effective Hamiltonian in Eq. (5), and take the form of

$$\begin{aligned} 1-\mathcal{F}_{\rm trans} &= 1-|\langle\psi_{\rm tar}||\psi(\frac{\pi}{2\lambda}+\delta t)\rangle|^2 \\ &\approx (|C_{eg}|^2+|C_{ge}|^2+2|C_{ee}|^2)^2(\lambda\delta t)^2, \end{aligned} \tag{20}$$

where δt is a small deviation of the interaction time. Moreover, the error in generating the AMES can be expressed as

$$\begin{aligned} 1-\mathcal{F}_{224} &= 1-|\langle\psi_{224}||\psi(\frac{\pi}{4\lambda}+\delta t)\rangle|^2 \\ &\approx 1-\frac{1}{4}[1+\cos(2\lambda\delta t))]^2\approx 2(\lambda\delta t)^2. \end{aligned} \tag{21}$$

4.2. The asymmetric coupling

If the electric field strength of the cavity modes are not identical, another important source of error is the asymmetric coupling due to the difference of $g_{\rm A}$ and $g_{\rm B}$, leading to $\lambda_{\rm A}\neq\lambda_{\rm B}$. Assuming that $\lambda_{\rm A}=\lambda_0+\delta\lambda/2$ and $\lambda_{\rm B}=\lambda_0-\delta\lambda/2$, where $\delta\lambda$ is a small value, the error for transferring an arbitrary quantum state encoded on the two qubits takes the form of

$$\begin{aligned} &1-\mathcal{F}_{\rm asy,trans} \\ &= 1-||C_{gg}|^2+|C_{eg}|^2\,{\rm e}^{-{\rm i}\delta\lambda\pi/(4\lambda_0)}\sin[(\lambda_0+\delta\lambda/2)\pi/(2\lambda_0)] \\ &\quad +|C_{ge}|^2\,{\rm e}^{{\rm i}\delta\lambda\pi/(4\lambda_0)}\sin[(\lambda_0-\delta\lambda/2)\pi/(2\lambda_0)] \\ &\quad +\frac{|C_{ee}|^2}{2}[1+\cos(\delta\lambda\pi/(2\lambda_0))]|^2 \\ &\approx 1-\left[\frac{|C_{ee}|^2}{2}+(|C_{eg}|^2-|C_{ge}|^2)^2\right]\left(\frac{\delta\lambda\pi}{4\lambda_0}\right)^2. \end{aligned} \tag{22}$$

Surprisingly, to generate the AMES with asymmetric coupling, the fidelity at $t=\pi/(4\lambda_0)$ reads

$$\begin{aligned} \mathcal{F}_{\rm asy,224} = \Bigg|\frac{\rm i}{2}\Bigg[&\left(\cos\lambda_0\frac{\pi}{4\lambda_0}-\cos\frac{\delta\lambda\pi}{8\lambda_0}\right) \\ &+\left({\rm i}\sin\lambda_0\frac{\pi}{4\lambda_0}-{\rm i}\sin\frac{\delta\lambda\pi}{8\lambda_0}\right) \\ &+\left({\rm i}\sin\lambda_0\frac{\pi}{4\lambda_0}+{\rm i}\sin\frac{\delta\lambda\pi}{8\lambda_0}\right) \\ &+\left(\cos\lambda_0\frac{\pi}{4\lambda_0}+\cos\frac{\delta\lambda\pi}{8\lambda_0}\right)\Bigg]\Bigg|^2=1, \end{aligned} \tag{23}$$

which means the generation of the AMES is robust to the asymmetric coupling. In the double-excitation subspace, eigenenergies of the effective Hamiltonian are $\lambda_{\rm A}+\lambda_{\rm B}$ and $2(\lambda_{\rm A}+\lambda_{\rm B})$. Adopting definitions $\lambda_{\rm A}=\lambda_0+\delta\lambda/2$ and $\lambda_{\rm B}=\lambda_0-\delta\lambda/2$, the eigenenergies remain $2\lambda_0$ and $4\lambda_0$, which ensures the robustness of the system.

4.3. The decoherence of the system

In the far-detuning regime, the requirement on the quality factor is relaxed, because the qubit–ququart interaction is realized by the virtual-photon exchange. The cavity is excited in low probability $P\propto(g/\Delta)^2$, and the effective lifetime of the photons is prolonged. For the state transfer, the fidelity will be affected by the photonic lifetime $1/\kappa$, the atomic excited lifetime $1/\gamma$, the total excitation N and the detuning Δ. As the detuning increases, the interaction time could be comparable with the excited lifetime of atoms. Dynamics of the entire system with decoherence can be described by the dissipative quantum master equation, which can be expressed as follows:

$$\begin{aligned} \frac{\rm d}{{\rm d}t}\rho &= -{\rm i}[H,\rho]+\kappa\mathcal{D}(a)\rho+\kappa\mathcal{D}(b)\rho \\ &\quad +\gamma[\mathcal{D}(\sigma_{\rm A})\rho+\mathcal{D}(\sigma_{\rm B})\rho+\mathcal{D}(|1\rangle\langle 2|)\rho+\mathcal{D}(|1\rangle\langle 3|)\rho \\ &\quad +\mathcal{D}(|2\rangle\langle 4|)\rho+\mathcal{D}(|3\rangle\langle 4|)\rho], \end{aligned} \tag{24}$$

where $\mathcal{D}(O)\rho=O\rho O^\dagger-(O^\dagger O\rho-\rho O^\dagger O)/2$ represents the dissipative superoperator.

For example, a cavity QED system consisting of three atoms within a high-Q microwave cavity can obtain single-atom coupling constant $g=2\pi\times 24$ kHz,[59–61] and the resonance frequency of the cavity is about 50 GHz. With the choice of $\Delta=10g$, the interaction time for the state transfer is $\pi/(2g^2/\Delta)=1\times10^{-4}$ s, which is much faster than the excited lifetime $1/\gamma=3\times10^{-2}$ s[59–61]. For a cavity with quality factor $Q=10^7$ and decay rate $\kappa=0.2g$ resulting in a cooperativity $C=g^2/(2\kappa\gamma)=10^4$, the effective lifetime is 3×10^{-3} s much larger than the interaction time. The fidelity for state transfer of $(1|gg\rangle+2|ge\rangle+3|eg\rangle+4|ee\rangle)/\sqrt{30}$ is approximately 0.97. Using a cavity with $Q=10^8$, the fidelity can exceed 0.98.

Furthermore, the choice of the far-detuning condition can efficiently generate the maximal entanglement among the three atoms, while in the resonant case, the atoms become highly entangled with the cavity fields during the evolution.

The result of the master equation is depicted in Fig. 6. As the detuning is not so large, the decoherence of the cavity significantly affects the fidelity of the state preparation. With a set of parameters discussed above, i.e., $\kappa=0.2g$ and $\gamma=2.2\times10^{-4}g$ ($Q=10^7$ and $C=10^4$), the maximal entangled state is generated at $t=\pi/(4\lambda)$ with fidelity of $\mathcal{F}=0.969$ and 0.975 as the detuning $\Delta=20g$ and $50g$, respectively, as shown in Fig. 6(a). As the detuning increases, the influence of photonic decay will weaken. A cavity with a higher quality factor can improve the fidelity, as depicted in Fig. 6(b)

with $\kappa = 0.02g$ ($Q = 10^8$ and $C = 10^5$). The fidelity $\mathcal{F}$ is larger than 0.985 with detuning $\Delta = 10g$, and it still exceeds 0.975 with detuning $\Delta = 20g$. However, the interaction time is larger, and the decoherence of atoms affects the preparation, as shown by the case of $\Delta/g = 50$. Furthermore, another consideration is that three atoms are placed into an optical cavity whose resonance wavelength is in the region of 630 nm–850 nm.[62–64] The system with predicted parameters $(g,\ \kappa,\ \gamma)/2\pi = (700,\ 3.5,\ 2.62)$ MHz ($Q \approx 10^8$) can achieve state transfer and generation of the AMES with fidelity more than 0.939 as $\Delta = 10g$, while fidelity decreases to 0.89 in the case of $\Delta = 20g$. In the experiment, to achieve high fidelity state transfer and entanglement generation, a suitable detuning should be determined by considering both the cavity's quality factor and the coherence time of atoms.

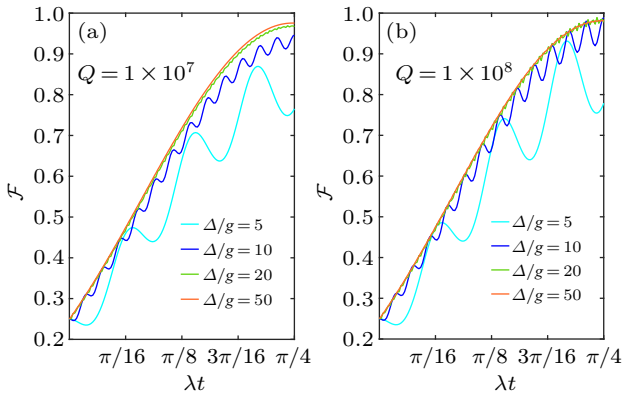


Fig. 5. The time evolution of the fidelity for preparing the (2, 2, 4) entangled state, with (a) the quality factor $Q = 10^7$ and the atom decay rate $\gamma = 2.2 \times 10^{-4} g$, and (b) the quality factor $Q = 10^8$.

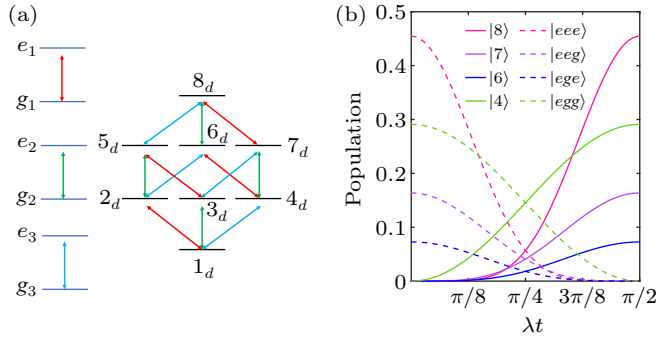


Fig. 6. (a) The level structure and transitions of three qubits and a qudit with eight eigenstates. (b) The transferring process of the population of qubit's state (dashed lines) and qudit's state (solid lines).

4.4. The generalization to the higher-dimensional case

This scheme can be expanded to higher-dimensional systems. Assume that there are N qubits constructing a 2^N-dimensional Hilbert space, and another single qudit hosts 2^N eigenstates. All of these N qubits and the qudit interact with the N-modes electromagnetic fields which are described by bosonic operators, a_n and $a_n^\dagger$. There are $M \equiv 2^{N-1}$ special transitions $\{J_{n,j}\}$ in the qudit interacting with the a_n field, and the collective transitions reads

$$D_n = |g_n\rangle\langle e_n| + \sum_{j=1}^{M} J_{n,j}. \tag{25}$$

The interaction between qubits, the qudit, and fields takes the form of

$$H_{\rm int} = g \sum_{n=1}^{N} (D_n^\dagger a_n + a_n^\dagger D_n). \tag{26}$$

This interaction Hamiltonian can implement the state transfer in the far-detuning regime, and the effective interaction with vacuum field modes can be written as

$$H_{\rm eff} = \lambda \sum_{n=1}^{N} D_n^\dagger D_n. \tag{27}$$

We can consider the specific case of three qubits and one qudit with $d = 8$. The level structure and the transitions of these particles are displayed in Fig. 7(a). The collective transition operators are given by

$$\begin{aligned} D_1 &= |g_1\rangle\langle e_1| + |1_d\rangle\langle 2_d| + |3_d\rangle\langle 5_d| + |4_d\rangle\langle 6_d| + |7_d\rangle\langle 8_d|, \\ D_2 &= |g_2\rangle\langle e_2| + |1_d\rangle\langle 3_d| + |2_d\rangle\langle 5_d| + |4_d\rangle\langle 7_d| + |6_d\rangle\langle 8_d|, \\ D_3 &= |g_3\rangle\langle e_3| + |1_d\rangle\langle 4_d| + |2_d\rangle\langle 6_d| + |3_d\rangle\langle 7_d| + |5_d\rangle\langle 8_d|, \end{aligned} \tag{28}$$

and they interact with field mode $a_1^\dagger$, $a_2^\dagger$, and $a_3^\dagger$, respectively. As shown in Fig. 7(b), the population of the three atoms can be transferred to the 8-level qudit at $t = \pi/(2\lambda)$, starting from the initial three-qubit state

$$\begin{aligned} |\psi_{0,\rm qbs}\rangle = \frac{1}{\sqrt{54}} \big(&5|e_3e_2e_1\rangle + 3|e_3e_2g_1\rangle \\ &+2|e_3g_2e_1\rangle + 4|e_3g_2g_1\rangle\big). \end{aligned} \tag{29}$$

We should note that while the interaction time remains $t = \pi/(2\lambda)$, the number of parameters in the Hamiltonian increases rapidly, making it more challenging to control them. An analysis on the decomposition of a qudit operator into multiple qubits[65] may be helpful for the generalization of qubit–qudit operations to the higher dimensional system.

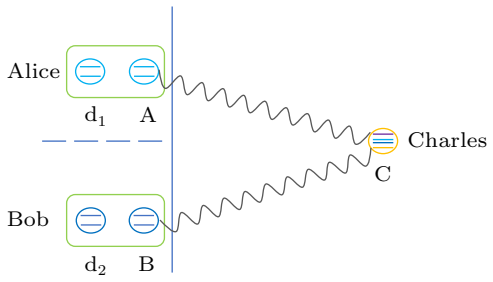


Fig. 7. Sketch of the quantum state teleportation from two uncorrelated qubits to a single ququart, and the asymmetric maximal entangled state serves as a communication channel.

4.5. Quantum teleportation between two qubits and a ququart

With the previous efficient preparation of the AMES, it is possible to make use of this entanglement channel to implement quantum state teleportation for atomic qubits and an

atomic ququart. Here, we introduce a potential quantum teleportation protocol based on the AMES[38] to teleport quantum information initially encoded on the two-qubit system to a ququart. First, two qubits, A and B, and a ququart C are coupled through a waveguide resonator.[66–68] After an appropriate time, they are prepared in the (2, 2, 4) entangled state, and then they are decoupled. Assume that Alice, Bob, and Charles hold qubit A, qubit B, and ququart C, respectively. Alice and Bob also hold qubits d_1 and d_2 of other qubits pair, whose unknown quantum state can be written as

$$\begin{aligned}|\phi\rangle_{d_1,d_2} &= c_1|gg\rangle_{d_1,d_2}+c_2|ge\rangle_{d_1,d_2}\\ &\quad +c_3|eg\rangle_{d_1,d_2}+c_4|ee\rangle_{d_1,d_2}.\end{aligned} \tag{30}$$

Before measurements and operations, the combined state of all above five particles is

$$\begin{aligned}&|\phi\rangle_{d_1,d_2}\otimes|\psi_{2,2,4}\rangle_{A,B,C}\\ =\ &|\Phi^+\rangle_{d_1,A}|\Phi^+\rangle_{d_2,B}(c_1|1\rangle_C+c_2|2\rangle_C+c_3|3\rangle_C+c_4|4\rangle_C)\\ &+|\Phi^+\rangle_{d_1,A}|\Phi^-\rangle_{d_2,B}(c_1|1\rangle_C-c_2|2\rangle_C+c_3|3\rangle_C-c_4|4\rangle_C)\\ &\cdots\\ &+|\Psi^-\rangle_{d_1,A}|\Psi^+\rangle_{d_2,B}(-c_4|1\rangle_C-c_3|2\rangle_C+c_2|3\rangle_C+c_1|4\rangle_C)\\ &+|\Psi^-\rangle_{d_1,A}|\Psi^-\rangle_{d_2,B}(c_4|1\rangle_C-c_3|2\rangle_C-c_2|3\rangle_C+c_1|4\rangle_C),\end{aligned} \tag{31}$$

where $|\Phi^\pm\rangle=(|gg\rangle\pm|ee\rangle)/\sqrt{2}$, and $|\Psi^\pm\rangle=(|ge\rangle\pm|eg\rangle)/\sqrt{2}$ are the two-body Bell states. Thus, to teleport the unknown state, Alice will perform the Bell measurement on qubit A and d_1 via two-qubit controlled gate,[35,66] while Bob will also perform the Bell measurement on qubit B and d_2. Their measurement results are sent to Charles, and based on the results, he applies some control fields on the ququart C to implement a 4-dimensional unitary operation,[69] and finally the quantum state of the ququart becomes

$$|\phi\rangle_C=c_1|1\rangle_C+c_2|2\rangle_C+c_3|3\rangle_C+c_4|4\rangle_C. \tag{32}$$

We can also expand this scenario to teleport a single ququart information to a pair of qubits via the (2, 2, 4) entangled state by employing 4-dimensional Bell measurement[70] on the source ququart and the entangled ququart. The measurement result determines the 2-dimensional unitary operation on qubits of the (2, 2, 4) entangled state.

In recent years, significant researches have been devoted to exploring high-dimensional teleportation,[71–73] which all focus on information transfer between particles in the same-dimensions. The protocol we introduced above utilizes a type of entangled states with asymmetric particle numbers, and allows state teleportation between multiple objects and a single object. It fundamentally differs from those schemes of high-dimensional quantum teleportation, as the latter implement the information transfer between individual particles.

5. Conclusion

We discuss the state transfer and the entanglement generation between 2- and 4-level atoms within a cavity to implement an information interface for quantum particles in different dimensions. We derive an effective qubit–ququart interaction with the far-detuning condition, which allows suppressed decoherence of the cavity. Our cavity QED scheme can obtain a high-fidelity transfer process for arbitrary two-qubit quantum states and its inverse efficiently, without measurements and post selections. Moreover, the proposed scheme can be made use of determinately preparing the atomic asymmetric maximally entangled state, and we find there is a bound of atomic coupling strength for generating the AMES in high fidelity. This high-fidelity preparation could be possibly applied in the quantum state teleportation between qubits and a ququart. The cavity QED would be a promising method to establish an interface for information communication between particles with different dimensions.

As a prospect, a quantum storage protocol is expected to be implemented, where the information from multiple qubits can be stored in a multi-level atom. Specifically, through Raman transitions, i.e., a combination of classical driving fields and multi-mode photonic channels,[21,74] multiple qubits' state will be transferred to multi-level atom's ground states, which allows a long lifetime of the storage. Multiple such high-dimensional atomic registers could be a promising platform for distributing quantum information in quantum networks. Furthermore, a non-local entanglement between qubits and qudits can be achieved in waveguide QED, where unidirectional coupling between quantum systems can prepare steady entangled states.[75,76] This cascaded architecture has potential for realizing quantum state teleportation in hybrid-dimensional systems.

Acknowledgments

Project supported by the National Natural Science Foundation of China (Grant No. 61974168), the National Key Research and Development Program of China (Grant No. 2017YFA0305200), and the Special Project for Research and Development in Key Areas of Guangdong Province of China (Grant No. 2018B030325001).

We thank Ze-Liang Xiang for very stimulating discussions. Part of the simulations are coded in MATLAB.

References

[1] O'Leary D P, Brennen G K and Bullock S S 2006 *Phys. Rev. A* **74** 032334

[2] Godfrin C, Ferhat A, Ballou R, Klyatskaya S, Ruben M, Wernsdorfer W and Balestro F 2014 *Phys. Rev. Lett.* **119** 187702

[3] Klimov A B, Guzman R, Retamal J C and Saavedra C 2003 *Phys. Rev. A* **67** 062313

[4] Sparrow C, Martin-Lopez E, Maraviglia N, Neville A, Harrold C, Carolan J, Joglekar Y N, Hashimoto T, Matsuda N and O'Brien J L 2018 *Nature* **557** 660

[5] Chi Y, Huang J, Zhang Z, *et al.* 2022 *Nat. Commun.* **13** 1162

[6] Niu M Y, Chuang I L, Shapiro J H, *et al.* 2018 *Phys. Rev. Lett.* **120** 160502

[7] Neeley M, Ansmann M, Bialczak R C, Hofheinz M, Lucero E, Connell A D O, Sank D, Wang H, Wenner J, Cleland A N, Geller M R and Martinis J M 2009 *Science* **325** 722

[8] Soltamov V, Kasper C, Poshakinskiy A, Anisimov A, Mokhov E, Sperlich A, Tarasenko S, Baranov P, Astakhov G and Dyakonov V 2019 *Nat. Commun.* **10** 1678

[9] Moreno-Pineda E, Godfrin C, Balestro F, Wernsdorfer W and Ruben M 2018 *Chem. Soc. Rev.* **47** 501

[10] Bullock S S, O'Leary D P and Brennen G K 2005 *Phys. Rev. Lett.* **94** 230502

[11] Lanyon B P, Barbieri M, Almeida M P, Jennewein T, Ralph T C, Resch K J, Pryde G J, O'brien J L, Gilchrist A and White A G 2005 *Nat. Phys.* **5** 134

[12] Ralph T C, Resch K J and Gilchrist A 2007 *Phys. Rev. A* **75** 022313

[13] Rico E, Dalmonte M, Zoller P, Banerjee D, Bogli M, Stebler P and Wiese U J 2018 *Ann. Phys.* **393** 466

[14] Gonzalez-Cuadra D, Zache T V, Carrasco J, Kraus B and Zoller P 2022 *Phys. Rev. Lett.* **129** 160501

[15] MacDonell R J, Dickerson C E, Birch C J, Kumar A, Edmunds C L, Biercuk M J, Hempel C and Kassal I 2021 *Chem. Sci.* **12** 9794

[16] Kraft T, Ritz C, Brunner N, Huber M and Guhne O 2018 *Phys. Rev. Lett.* **120** 060502

[17] Kues M, Reimer C, Roztocki P, *et al.* 2017 *Nature* **546** 622

[18] Cervera-Lierta A, Krenn M, Aspuru-Guzik A and Galda A 2022 *Phys. Rev. Appl.* **17** 024062

[19] Collins D, Gisin N, Linden N, Massar S and Popescu S 2002 *Phys. Rev. Lett.* **88** 040404

[20] Feng T, Xu Q, Zhou L, Luo M, Zhang W and Zhou X 2022 *Photonics Res.* **10** 2854

[21] Cirac J I, Zoller P, Kimble H J and Mabuchi H 1997 *Phys. Rev. Lett.* **78** 3221

[22] Kurpiers P, Magnard P, Walter T, *et al.* 2018 *Nature* **558** 264

[23] Sillanpaa M A, Park J I and Simmonds R W 2007 *Nature* **449** 438

[24] Liu T, Su Q P, Yang J H, Zhang Y, Xiong S J, Liu J M and Yang C P 2017 *Sci. Rep.* **7** 7039

[25] Luis F, Repolles A, Martinez-Perez M J, Aguila D, Roubeau O, Zueco D, Alonso P J, Evangelisti M, Camon A, Sese J, Barrios L A and Aromi G 2011 *Phys. Rev. Lett.* **107** 117203

[26] Blais A, Huang R S, Wallraff A, Girvin S M and Schoelkopf R J 2004 *Phys. Rev. A* **69** 062320

[27] Wineland D J, Monroe C, Itano W M, King B E, Leibfried D, Myatt C and Wood C 1997 *Phys. Scr.* **T76** 147

[28] Kasper V, Hebenstreit F, Jendrzejewski F, Oberthaler M K and Berges J 2017 *New J. Phys.* **19** 023030

[29] Domokos P, Raimond J M, Brune M and Haroche S 1995 *Phys. Rev. A* **52** 3554

[30] Ladd T and Yamamoto Y 2011 *Phys. Rev. B* **84** 235307

[31] Yang C P, Chu S I and Han S 2003 *Phys. Rev. A* **67** 042311

[32] Bennett C H, Brassard G, Crepeau C, Jozsa R, Peres A and Wootters W K 1993 *Phys. Rev. Lett.* **70** 1895

[33] Goyal S K, Boukama-Dzoussi P E, Ghosh S, Roux F S and Konrad T 2014 *Sci. Rep.* **4** 4543

[34] Zhang C, Chen J F, Cui C, Dowling J P, Ou Z Y and Byrnes T 2019 *Phys. Rev. A* **100** 032330

[35] Zheng S B and Guo G C 2000 *Phys. Rev. Lett.* **85** 2392

[36] Guo G P, Li C F, Li J and Guo G C 2002 *Phys. Rev. A* **65** 042102

[37] Guo G C and Zhang Y S 2002 *Phys. Rev. A* **65** 054302

[38] Zhou L, Xu Q, Feng T and Zhou X 2022 arXiv: 221200545 [quant-ph]

[39] Schrieffer J R and Wolff P A 1966 *Phys. Rev.* **149** 491

[40] Jagsch S T, Greif L A T, Reitzenstein S and Schliwa A 2019 *Phys. Rev. B* **99** 245303

[41] Bertet P, Osnaghi S, Milman P, Auffeves A, Maioli P, Brune M, Raimond J M and Haroche S 2002 *Phys. Rev. Lett.* **88** 143601

[42] Tang L, Tang J, Zhang W, Lu G, Zhang H, Zhang Y, Xia K and Xiao M 2019 *Phys. Rev. A* **99** 043833

[43] Sayrin C, Junge C, Mitsch R, Albrecht B, O'Shea D, Schneeweiss P, Volz J and Rauschenbeutel A 2015 *Phys. Rev. X* **5** 041036

[44] Xu Q, Fattal D and R G 2008 *Opt. Express* **16** 4309

[45] Morigi G, Franke-Arnold S and Oppo G L 2002 *Phys. Rev. A* **66** 053409

[46] Ou B Q, Liang L M and Li C Z 2009 *Opt. Commun.* **282** 2870

[47] Stowe M C, Peter A and Ye J 2008 *Phys. Rev. Lett.* **100** 203001

[48] Lodahl P, Mahmoodian S and Stobbe S 2015 *Rev. Mod. Phys.* **87** 347

[49] Poshakinskiy A V and Poddubny A N 2016 *Phys. Rev. A* **93** 033856

[50] He X L, Yang C P, Li S, Luo J Y and Han S 2010 *Phys. Rev. A* **82** 024301

[51] Waseem M, Irfan M and Qamar S 2012 *Physica C* **477** 24

[52] Li H, Ge G, Liao L and Feng S 2015 *Found. Phys.* **45** 198

[53] Mabuchi H and Doherty A C 2002 *Science* **298** 1372

[54] Osnaghi S, Bertet P, Auffeves A, Maioli P, Brune M, Raimond J M and Haroche S 2001 *Phys. Rev. Lett.* **87** 037902

[55] Fortier K M, Kim S Y, Gibbons M J, Ahmadi P and Chapman M S 2007 *Phys. Rev. Lett.* **98** 233601

[56] Imamog A, Awschalom D D, Burkard G, *et al.* 1999 *Phys. Rev. Lett.* **83** 4204

[57] Malik M, Erhard M, Huber M, Krenn M, Fickler R and Zeilinger A 2016 *Nat. Photonics* **10** 248

[58] Hu X M, Xing W B, Zhang C, Liu B H, Pivoluska M, Huber M, Huang Y F, Li C F and Guo G C 2020 *NPJ Quantum Inf.* **6** 88

[59] Raimond J M, Brune M and Haroche S 2001 *Rev. Mod. Phys.* **73** 565

[60] Lin G W, Ye M Y, Chen L B, Du Q H and Lin X M 2007 *Phys. Rev. A* **76** 014308

[61] Li Y H and Nie L P 2013 *Int. J. Theor. Phys.* **52** 961

[62] Shi Z C, Xia Y, Song J and Song H S 2013 *Quantum Inf. Process.* **12** 411

[63] Chen Z, Chen Y H, Xia Y, Song J and Huang B H 2016 *Sci. Rep.* **6** 22202

[64] Spillane S M, Kippenberg T J, Vahala K J, Goh K W, Wilcut E and Kimble H J 2005 *Phys. Rev. A* **71** 013817

[65] Suchowski H, Silberberg Y and Uskov D B 2011 *Phys. Rev. A* **84** 013414

[66] Steffen L, Salathe Y, Oppliger M, Kurpiers P, Baur M, Lang C, Eichler C, Puebla-Hellmann G, Fedorov A and Wallraff A 2013 *Nature* **500** 319

[67] Xiang Z L, Ashhab S, You J Q and Nori F 2013 *Rev. Mod. Phys.* **85** 623

[68] Hattermann H, Bothner D, Ley L, Ferdinand B, Wiedmaier D, Sárkány L, Kleiner R, Koelle D and Fortágh J 2017 *Nat. Commun.* **8** 2254

[69] Li Y C, Martinez-Cercos D, Martínez-Garaot S, Chen X and Muga J 2018 *Phys. Rev. A* **97** 013830

[70] Wang F, Erhard M, Babazadeh A, Malik M, Krenn M and Zeilinger A 2017 *Optica* **4** 1462

[71] Luo Y H, Zhong H S, Erhard M, Wang X L, Peng L C, Krenn M, Jiang X, Li L, Liu N L, Lu C Y, Zeilinger A and Pan J W 2019 *Phys. Rev. Lett.* **123** 070505

[72] Wang X L, Cai X D, Su Z E, Chen M C, Wu D, Li L, Liu N L, Lu C Y and Pan J W 2015 *Nature* **518** 516

[73] Hu X M, Zhang C, Liu B H, Cai Y, Ye X J, Guo Y, Xing W B, Huang C X, Huang Y F, Li C F and Guo G C 2020 *Phys. Rev. Lett.* **125** 230501

[74] Zheng S B 1998 *Quantum and Semiclassical Optics: Journal of the European Optical Society Part B* **10** 691

[75] Stannigel K, Rabl P and Zoller P 2012 *New J. Phys.* **14** 063014

[76] Pichler H, Ramos T, Daley A J and Zoller P 2015 *Phys. Rev. A* **91** 042116